Indian Make Portable and Real-time Shearography System (IMPRESS) for Non-Destructive Testing (NDT)

Digendranath Swain [0000-0003-3325-1597], Binu P Thomas, S K Selvan, and Jeby Philip

Experimental Mechanics Division, Structural Testing Group, Structural Engineering Entity, Vikram Sarabhai Space Centre, ISRO P.O., Thiruvananthapuram, Kerala, India, 695 022
digendranath@gmail.com

Abstract. Laser shearographic interferometry is a well-proven NDT technique for detecting defects in various structures and mechanical components. There is only countable number of shearography systems available commercially. This paper highlights the development of an indigenous low-cost digital laser shearography system namely IMPRESS (Indian Make Portable and Real-time Shearography System). Herein, the details of the system are explained with its on-line and in-situ capability. Moreover, a few specimen level results are shown to demonstrate the application of the system. The developmental cost of this system is much lower as compared to the commercial systems. Therefore, it would be beneficial for small and medium scale Indian industries who are desirous of using shearography as an NDT tool in their production line. Currently, the system is being upgraded to make it on par with other commercial systems.

Keywords: Laser speckle, Shearing interferometry, Shearography, Defects, In-situ NDT, Digital shearography.

1 Introduction

Laser speckle shearography is a coherent non-contact whole-field optical interferometry technique that measures derivatives of surface displacement fields of an object under external stress. The loci of deformation derivatives are mapped as fringe patterns known as shearograms. Shearography was originally proposed by Hung in 1982 [1] who recorded specklegrams in photographic films. He visualized the fringe patterns through high pass optical Fourier filtering setups. Subsequently, Steinchen and Yang [2-3], used digital cameras and image processing methods for visualizing the shearographic fringe patterns. The induction of digital cameras as a recording media enabled substantial growth of shearography as a robust NDT technique. Over the years a few commercial digital shearography systems have been developed and introduced into the market as a non-destructive inspection (NDI) tool [4]. In India, especially in the automobile, aerospace and defense sector, a few such systems are currently in use for regular NDT purpose. The price of these commercial shearography NDT systems is significantly high. Therefore, Indian medium or small-scale industries have difficulty in implementing such systems into their production line for quality control or NDT purpose. Towards this, a shearography system development was

initiated by the authors at Vikram Sarabhai Space Center, ISRO, aiming at developing a cost effective portable shearography system with an area of coverage up to 1 square meter. The system is mainly targeted for in-situ and on-line NDT of metallic and composite structures including adhesively bonded sandwich metallic/composites.

2 Principle of Digital Shearography

When an object surface, with surface roughness of one order higher than the laser wavelength, is illuminated with a coherent laser, grainy speckle pattern is formed on the surface. When this speckle pattern is imaged through an optical lens, then it is called a subjective speckle pattern. Such grainy patterns can be recorded in the image plane of a digital camera. Speckle pattern generated on the object surface is due to the interference of the diffusively scattering light from neighboring points on its surface. The interference at a point carry random phase and amplitudes due to the random nature of scattering. The size of the subjective speckle pattern primarily depends mainly on the (i) aperture of the imaging system, (ii) magnitude of surface roughness, and (iii) the distance between the object and imaging system among other factors. Shearography is based on the principle of speckle interferometry where a reference speckle pattern is made to interfere with another speckle pattern imaged with a slight spatial shift. Therefore, two neighboring points on the object are made to interfere at the image plane of a digital sensor through a shearing optics (Fig. 1). Figure 1 shows an object illuminated with a laser source. The shearing optics as shown in Fig. 1 is a Michelson's interferometer wherein two images are formed through tilting the mirror in one of the arms of this interferometer. The angle of tilt of the mirror creates the lateral shift called the **shear amount**. The interference of the two speckle patterns at the image sensor is called a **specklegram** (Fig. 2(a)). Likewise, a deformed specklegram can be recorded in the image sensor after loading the object. Point to point digital subtraction of the two specklegrams would modulate the object intensity with fringe patterns. These fringe patterns are the loci of the surface displacement derivatives and these modulated intensity map is called as **shearogram** (Fig. 2(b)).

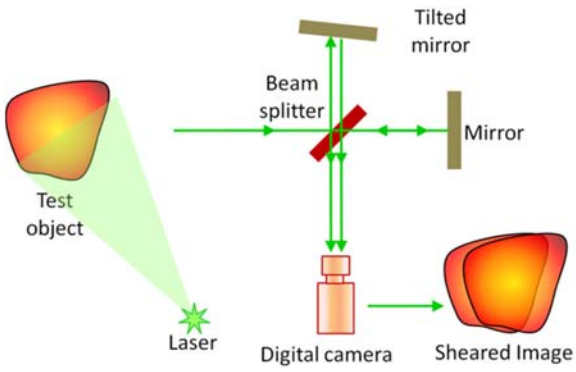

Fig. 1. Optical arrangement of a digital speckle shearography system

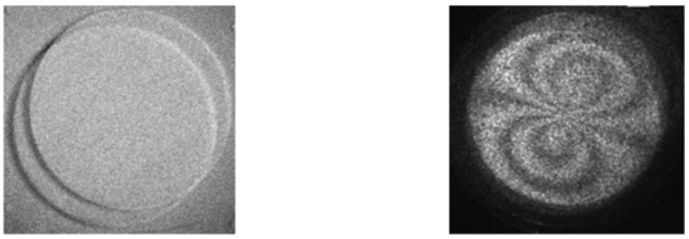

(a) (b)

Fig. 2. (a) Specklegram of a disc shaped object after interference of two speckle patterns and (b) shearogram of the same object obtained after digital subtraction of a reference specklegram from a deformed specklegram. Here, the shear amount is given in the diagonal direction.

2.1 Mathematical Description

Let $U(x,y) = a_1 e^{-i\phi_1}$ and $U(x+\delta x, y) = a_2 e^{-i\phi_2}$ be the complex amplitude of the speckle generated on the object at a point (x,y) and $(x+\delta x, y)$, respectively. Here, δx is the **shear amount**, $a_1 = a(x,y)$ and $a_2 = a(x+\delta x, y)$ are the amplitudes, $\phi_1 = \phi(x,y)$ and $\phi_2 = \phi(x+\delta x, y)$ are the random phases, respectively. When these speckle patterns interfere optically, they generate a specklegram. Let I_U be the intensity of the specklegram of an unloaded state of object, given as

$$I_U = (U(x,y) + U(x+\delta x, y))(U(x,y) + U(x+\delta x, y))^*, \tag{1}$$

where $()^*$ represents the complex conjugate operation. Equation (1) after simplification provides the following expression for I_u

$$I_U = (a_1^2 + a_2^2) + 2a_1 a_2 \cos(\phi_2 - \phi_1) = A + B\cos(\delta\varphi), \tag{2}$$

where $\delta\varphi(x,y) = \phi_2 - \phi_1$ is the random interference phase between the two speckle patterns, $A = (a_1^2 + a_2^2)$ and $B = 2a_1 a_2$, respectively.

Let Δ be the relative phase change between two neighboring points due to the relative displacement of these two points due to loading. Considering I_L as the intensity of the specklegram of the object after loading, I_L can be written as [3]

$$I_L = A + B\cos(\delta\varphi + \Delta). \tag{3}$$

In digital shearography, the pixel by pixel digital subtraction of the intensities in Eqs. (2) and (3) results into a shearogram which is mathematically written as [6]

$$I = \left| B[\cos(\delta\varphi + \Delta) - \cos(\delta\varphi)] \right| = B\sin\left(\phi + \Delta/2\right)\sin(\Delta/2). \tag{4}$$

The relative phase difference Δ for normal illumination and viewing direction with horizontal lateral shift is given as [3]

$$\Delta = \frac{4\pi}{\lambda}\frac{dw}{dx}\delta x \tag{5}$$

where dw/dx is derivative of the out of plane displacement along x direction and λ is the wavelength of laser source used. When $\Delta/2$ in $\sin(\Delta/2)$ becomes integral multiple of 2π, intensity becomes zero resulting in black fringes. Herein, only x-direction shearing is illustrated for simplicity. However, such shearing in y-direction or a combination of x and y can be provided. The shearogram in Fig. 2(b) shows such a combined shearing.

2.2 Michelson's Interferometer with 4-f Imaging

The size of the object to be imaged using the optical setup shown in Fig. 2 is limited by the size of the optical elements and the imaging lens. Hence to increase the coverage area Michelson's interferometer is modified with 4f imaging optics [5] as shown in Fig. 3. Here the imaging lens and image sensor are placed separated unlike conventional digital shearography system. The imaging lens is the first optical element in this modified setup whereas beam splitter is first element in the conventional Michelson's setup. The imaging lens focuses the object at its focal plane and the first 4f imaging lens is kept at the focal plane of this imaging lens. The second 4-f imaging lens is kept at 2f distance from the first one as shown in Fig. 3. Finally, the CCD/image sensor is kept at the focal plane of the second 4-f imaging lens. Thus large objects can be viewed through this setup. The angle of view can further be increased by replacing lens with smaller focal length. Moreover this setup facilitates use of small beam splitter and mirrors. Hence, it can be utilized for developing miniaturized systems.

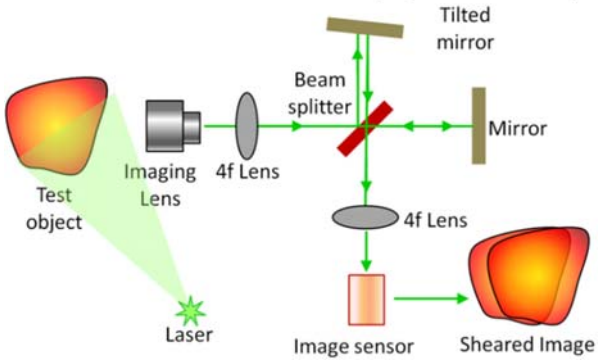

Fig. 3. Modified Michelson's interferometer with 4-f imaging optics.

3 Development of IMPRESS

We have initially developed a bread-board model for checking the shearograms generated from a trial 4-f setup. During this period, a LABVIEW code was developed for visualizing the shearograms. Subsequently, a portable optical head was configured and fabricated for in-situ and portable utility. This section provides these details.

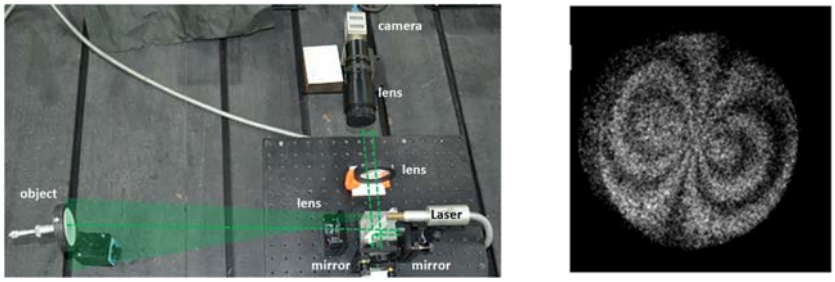

(a) (b)

Fig. 4. (a) Bread-board model 4-f optical setup for trial experiments and (b) resulting shearogram for a disc loaded at the center.

3.1 Demonstration with Bread-board Model

A bread-board setup using Michelson's interferometer with 4-f imaging optics was made on a vibration isolation table. Trial experiments were carried out as shown in the setup in Fig. 4(a). Here the imaging lens was integrated with the image sensor. A 6W VERDI laser at maximum power level of 1 W was used in all the experiments with an optical fiber for guiding the beam. The resulting real-time shearogram for disc loaded at the center is shown in Fig. 4(b).

Fig. 5. Front end of the real-time software of IMPRESS (version 0)

3.2 Development of Software for IMPRESS

A front-end software was developed in LabVIEW platform to (i) acquire the specklegram in real time, (ii) store reference specklegram at any stress state, (iii) generate shearogram through pixel to pixel digital subtraction between the reference specklegram and (iv) recoding of live specklegram at current stress state. The front screen of the software is shown in Fig. 5 where each window respectively displays live specklegram, chosen reference image and shearogram in real time. The reference image can be changed in real-time to obtain clear shearograms. The software was developed to acquire specklegrams using PixeLINK CMOS camera. Feature for selecting any region of interest (ROI) and controls for acquisition speed and exposure time are provided in the software. Full frame size of 3000 × 2208 pixels at 5 fps can be recorded. The outputs shearograms can be saved in image format and video formats.

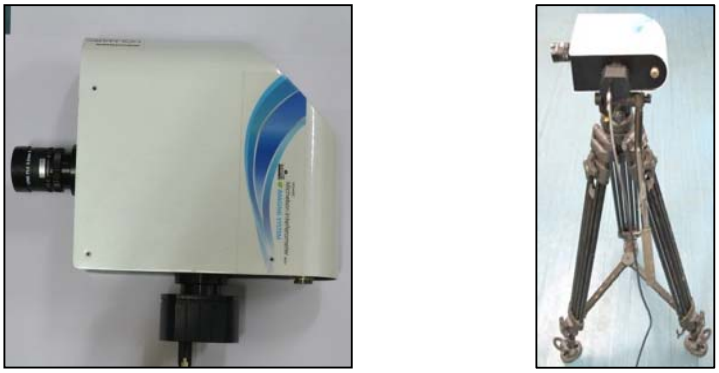

(a) (b)

Fig. 6. (a) The shearographic head housing the 4-f imaging optics and (b) the optical head mounted on a tripod for in-situ application.

3.3 Development of Proto Optical Head for In-situ and On-line NDT

A compact unit was later designed to accommodate 4f imaging lenses, mirror with tilt control on a translation stage, beam splitter plate, imaging lens and image sensor. An enclosure was fabricated for assembling all the optical elements inside it as shown in Fig. 6(a). Provision was made in the system to replace the fixed plane mirrors in the two arms of Michelson's interferometer with piezo actuated mirrors. One piezo mirror is for computerized control for shear amount and other one is for phase shifting of one arm at λ/4 steps. Therefore, four phase-shifted shearograms can be recorded to generate phase map for quantifying displacement derivative. The shearing camera as mounted on a tripod is shown in Fig. 6(b) which was used for in-situ tests.

4 Results Demonstrating IMPRESS

In this section, salient results obtained from the fabricated prototype would be presented to demonstrate IMPRESS. Initially, we present the results obtained with vibration testing followed by the results obtained using thermal stressing.

4.1 Results from Vibration Testing

Preliminary experiments were carried out on a honeycomb sandwich specimen with Aluminium face sheets of size 300 mm x 100 mm with two programmed skin sheet debonds (marked squares in the specimen in Fig. 7(a)). One edge of the specimen was clamped using a vice and vibration stressing was applied using a piezo shaker (Fig. 7(b)). The piezo shaker was mounted on the specimen using a vacuum cup. Shearogram of the panel with fringe patterns representing loci of displacement derivatives due to the local resonance of the debonded region is shown Fig. 7(c).

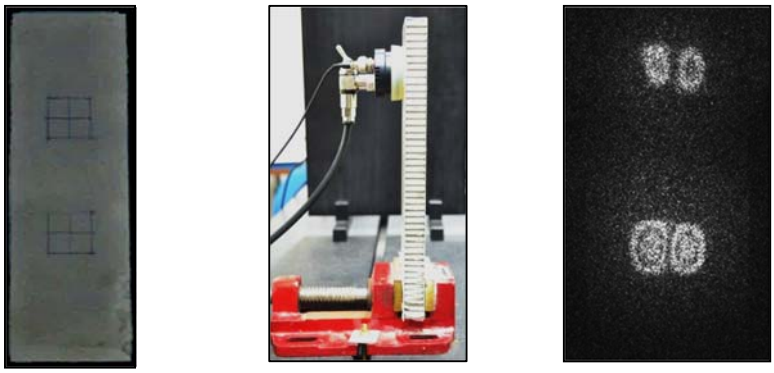

(a) (b) (c)

Fig. 7. (a) Honeycomb specimen, (b) experimental setup with piezo shaker and (c) shearogram of the defects during vibration.

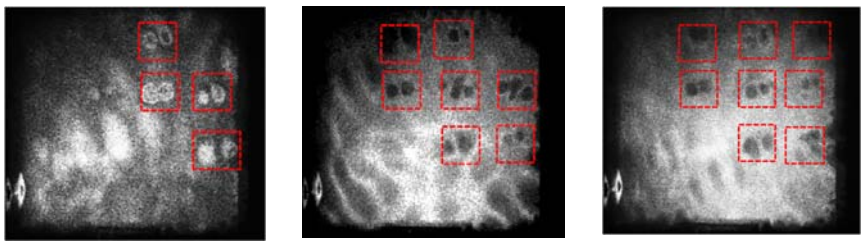

(a) (b) (c)

Fig. 8. Programmed defects on a honeycomb sandwich panel of different sizes identified at different frequencies.

Using the same clamp and the piezo shaker setup, another 300 mm by 300 mm honeycomb sandwich panel, containing nine programmed defects of various sizes, was tested. The identified defects at different frequencies are shown in Fig. 8, wherein almost 8 defects could be identified. Only the smallest defect could not be identified with the setup used. The system response and sensitivity needs further improvement.

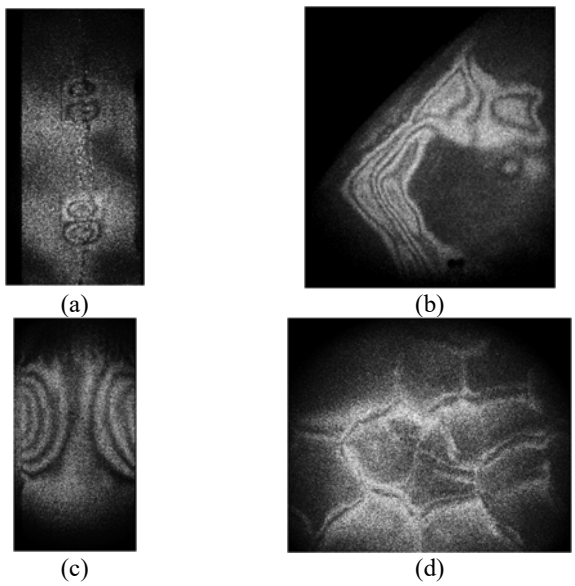

Fig. 9. Shearogram of (a) the same honeycomb panel in Fig. 7, (b) debond on a satellite adaptor made of metallic honeycomb, (c) debond of a skin sheet of a carbon-epoxy honeycomb panel, and (d)) cracks in a silica tile obtained using IMPRESS under thermal loading.

4.2 Results from Thermal Stressing

Vibration stressing is mostly limited to identification of debonds and delamination. But defects like inclusions, cracks, and voids are mostly sensitive to thermal stressing. Shearograms of the same defects of Fig. 7 on the sandwich panel could be captured using an ice cube as a thermal source (see Fig. 9(a)). Cracks in a silica tile specimen also could be obtained by heating a sample using an infrared light source (Fig. 9(b)). A skin debond in a honeycomb sandwich panel with carbon epoxy skin sheets also could be identified under thermal stressing (Fig. 9(c)). The object in Fig. 9(d) is a conical satellite adapter made of metallic honeycomb sandwich with thin aluminum face sheets of size around 0.5 m with programmed face sheet debonds. The skin debond also could be identified under minimal thermal stressing. In all of the above examples, the region, size and shape of the defects are clearly identifiable from the fringe patterns. Since fringes are confined to only defective regions, defect identification is very easy compared to holography technique.

5 Concluding Remarks

A prototype of a portable shearographic head was developed in-house for NDT of various structures and components. The shearing camera is developed based on a modified Michelson's interferometer with a 4f imaging system to increase the area of coverage. The resulting system with its software is named as the Indian Make Portable and Real-time Shearography System (IMPRESS). The inclusion of 4-f optics enhanced the capability of IMPRESS to image 1 square meter objects for identifying defects. However, depending upon the sensitivity and size of the defect the area of coverage must be optimized during in-situ tests. At this stage, the system is tuned to work under mechanical, vibration and thermal stressing methods. This system can be used with vacuum stressing also. The NDT results obtained are very encouraging. A lot of expertise is gained through the development of the system and the technological know-how. The current capability of the system would be sufficient for NDT of various engineering components. Moreover, the system can be explored further for various defects in metallic and composite structures such as weld defects, brazing anomalies, and other honeycomb defects. Furthermore, the system can be used for investigating structural integrity of pressure vessels, thermal protection systems and other engineering components. Further work to automate the system is in progress so that sophistications at par with commercial systems can be built into the system.

Acknowledgements. The authors wish to acknowledge Shri N Shyam Mohan, Group Director/STG, VSSC and Shri M Premdas, Deputy Director/STR, VSSC for their encouragement. The authors would like to thank Mr S N Suresh, Sr. Techncian B, EXMD/VSSC for his relentless support during the experiments.

References

1. Hung, Y.Y.: Shearography a new optical method for strain measurement and non-destructive testing. Optical Engineering 21(3), 213391 (1982).
2. Steinchen, W., Yang, L.X., Schuth, M.: TV-shearography for measuring 3D-strains. Strain 32(2), 49-58 (1996).
3. Steinchen, W., Yang, L.X.: Digital shearography: Theory and application of digital speckle pattern shearing interferometry. SPIE Press monograph Vol. PM100, SPIE Press, Bellingham, Washington, USA (2003).
4. ASTM standard E 2581-07, Standard practice for shearography of polymer matrix composites, sandwich core materials and filament wound pressure vessels in aerospace applications, October (2007).
5. Wu, S., He, X., Yang, L.X.: Enlarging the angle of view in Michelson interferometer based shearography by embedding a 4f system. Applied optics 50 (21), 3789-3794 (2011).
6. Yang, L.X., Xie, X.: Digital shearography: New developments and applications. SPIE Press monograph Vol. PM267, SPIE Press, Bellingham, Washington, USA (2016).